

The Influence of Outer Hair Cells on Tectorial Membrane Waves

Haruki Mizuno¹, Toshiaki Kitamura^{1*}

¹Kansai University, Osaka, Japan

Abstract

The cochlea, a vital structure for hearing, comprising the scala media, scala tympani, and scala vestibuli, separated by Reissner's and basilar membranes. The scala media houses the organ of Corti, containing inner and outer hair cells (IHCs and OHCs). Extensive research has explored OHCs, focusing on their mechanical properties and role in cochlear mechanics. This study investigates the impact of OHCs on two types of tectorial membrane (TM) slow waves, termed TM wave 1 and TM wave 2, using modal analysis. The research utilizes a model incorporating the basilar membrane, TM, and OHCs. The study explores how OHCs influence the propagation characteristics of these waves. Results demonstrate that OHCs affect TM wave 1 minimally, with distinctions becoming negligible at higher frequencies. In contrast, OHCs significantly influence TM wave 2, especially in the high-frequency range. The study further explores the frequency-dependent phase and attenuation constants of these waves, revealing substantial effects of OHCs on TM wave 2 across different frequencies and TM widths. (**International Journal of Biomedicine. 2025;15(3):523-526.**)

Keywords: cochlea • outer hair cell • tectorial membrane • modal analysis • propagation characteristics

For citation: Mizuno H, Kitamura T. The Influence of Outer Hair Cells on Tectorial Membrane Waves. International Journal of Biomedicine. 2025;15(3):523-526. doi:10.21103/Article15(3)_OA10

Abbreviations

IHCs, inner hair cells; **OHCs**, outer hair cells; **TM**, tectorial membrane.

Introduction

The cochlea, a snail-shaped structure located in the inner ear, plays a crucial role in the process of hearing. It has three fluid-filled sections, namely the scala media, scala tympani, and scala vestibuli. These three compartments are separated by Reissner's membrane and the basilar membrane. The scala media, also known as the cochlear duct, contains a specialized structure called the organ of Corti. This complex organ is situated between the vestibular and tympanic ducts within the cochlea. The organ of Corti contains rows of outer hair cells (OHCs) and inner hair cells (IHCs). The IHCs are the primary sensory organs of the auditory system. They transduce the vibration of sound into electrical activity in nerve fibers, which is transmitted to the brain. The OHCs play a central role in signal amplification. They are directly coupled to the tectorial membrane (TM) via their hair bundles.

Extensive scientific inquiry has been directed towards understanding outer hair cells and their role in auditory processes.¹⁻⁶ Spector et al.¹ investigated the passive and

active properties of the cochlear OHC, providing insights into its mechanical characteristics, including Young's moduli, Poisson's ratios, and bending stiffness. They also examined the cell's active behavior, determining coefficients of active force production and limiting parameters of the electromotile response. Their findings contribute to modeling cochlear mechanics at the organ level. Tolomeo et al.² studied mammalian outer hair cells and their deformation mechanism and investigated the cortical cytoskeleton's role in directing cell deformation. They found that the cortical lattice exhibited differential stiffness, and the plasma membrane contributed significantly to cell stiffness. Karavitaki et al.³ investigated the role of OHC somatic motility in cochlear micromechanics and its impact on hearing sensitivity. Using a cochlear preparation, they observed significantly greater motion in OHCs, Deiter's cells, and Hensen's cells than in other structures. Dewey et al.⁴ examined the influence of bundle stiffness and the attachment of the TM on cochlear vibrations and their contribution to auditory sensation. Through the study of

mutant mice with reduced bundle stiffness or detached TM, the researchers discovered that decreased bundle stiffness led to a narrowing of tuning and a reduction in the high-frequency range of vibratory responses.

The previous studies have shown that there are two types of TM slow waves, which we refer to as TM wave 1 and TM wave 2.^{2,8} Figure 1 illustrates the TM displacement of (a) TM wave 1 and (b) TM wave 2, respectively, when $f = 10$ kHz. The amplitude and direction of the displacement are depicted by the vectors. The displacement of TM wave 1 is primarily located at the limbal attachment zone of TM, while the displacement of TM wave 2 is concentrated at the tip of the main body of TM at a high frequency ($f = 10$ kHz).

This study investigated the influence of OHCs on the two types of TM waves using modal analysis. We considered an analysis model composed of the basilar membrane, TM, and OHCs. The analysis model without the OHCs was also utilized for comparison. Here, we discuss how the OHCs affect the propagation characteristics of the two types of TM waves.

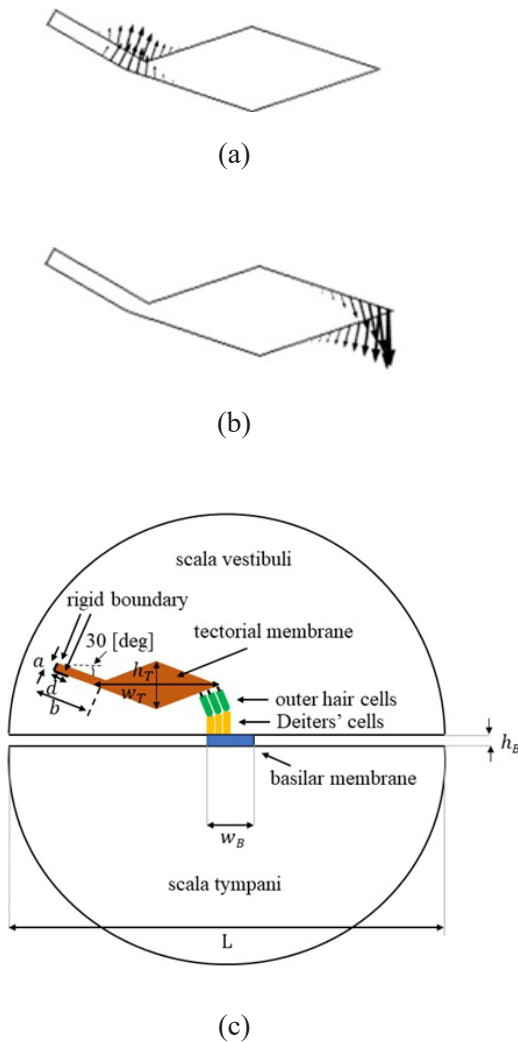


Fig. 1. TM displacement of (a) TM wave 1 and (b) TM wave 2, and (c) analysis model.

Materials and Methods

The organ of Corti sits between the TM and the basilar membrane, housing three rows of OHCs as shown in Fig. 1(c). This study examined how OHCs affect the waves on the TM. We used Comsol Multiphysics, a finite element method-based software, to analyze TM wave properties such as phase and attenuation constants. Each OHC is supported by Deiters' cells and has stereocilia on top. Deiters' cells are on the basilar membrane, and stereocilia attach to the TM above. Both OHCs and Deiters' cells have a Young's modulus of 3 kPa, while stereocilia have a Young's modulus of 100 kPa.² The basilar membrane parameters are fixed: width (w_B) = 0.3 mm, thickness (h_B) = 5 μ m, and Young's modulus (E_B) = 26.5 MPa.¹⁰ The Young's modulus (E_T) of the TM is 50 kPa.² The limbal attachment zone and the spiral limbus are firmly fastened, modeled as a rigid boundary ($d = 30$ μ m, $a = 10$ μ m, $b = 50$ μ m). We varied the width (w_T) of TM as a parameter. Here, the ratio between the width (w_T) and thickness (h_T) is fixed as $w_T = 3h_T$. The chamber radius remains constant at $r = 0.5$ mm. Both the TM and basilar membrane possess Poisson's ratio of 0.49 and a density of 1.2×10^3 kg/m³.^{11,12} The fluid possesses a bulk modulus of 2.2×10^9 Pa, a density of 1.034×10^3 kg/m³, and a viscosity of 2.8×10^{-3} Pa·s.^{11,12}

Results and Discussion

Figure 2 displays the frequency characteristics of phase constants and attenuation constants for TM wave 1 and TM wave 2, including the results of the analysis model in which the OHCs are excluded. As shown in Fig. 1(a), the TM wave 1 field concentrates in the limbal attachment zone, intensifying in the high-frequency range. Consequently, in the phase characteristics depicted in Fig. 2(a), differences based on the presence or absence of OHCs are minimal. As the frequency increases, these distinctions become almost negligible. In contrast, Fig. 1(b) illustrates the TM wave 2 field focusing on the tip of the TM main body. Thus, in the phase characteristics of Fig. 2(b), the influence of OHCs is prominent across all frequency domains, especially in the high-frequency range where the field concentration is significant, leading to substantial differences based on the presence or absence of OHC. Fig. 2(c) makes it evident that the influence of OHCs on the attenuation constants of TM wave 1 is remarkable in the lower frequency region compared to the phase constants shown in Fig. 2(a). As the frequency increases, the influence diminishes because the field concentrates in the limbal attachment zone, as mentioned above. Conversely, the influence on the attenuation constants of TM wave 2 becomes more pronounced with increasing frequency, as shown in Fig. 2(d). This is due to the TM wave 2 field becoming more concentrated at the tip of the TM main body. In most cases, OHCs have the effect of decreasing attenuation constants.

The phase and attenuation constants of TM wave 1 and TM wave 2, dependent on the width (w_T) of the TM, are depicted in Figure 3. Here, the ratio between the width (w_T) and thickness

(h_T) is fixed at $w_T = 3h_T$. We chose the acoustic frequencies for this analysis as $f = 5$ and 10 kHz. Fig. 3(a) shows that when $f = 10$ kHz, the phase constants of TM wave 1 are hardly affected by the presence or absence of OHCs, regardless of the TM width. In contrast, when $f = 10$ kHz, they are strongly affected for low frequency, and the influence of OHCs becomes stronger as the TM width decreases because the field concentration weakens and spreads to the OHCs due to the lower frequency and the smaller TM size. Fig. 3(b) illustrates that the influence of OHCs on the phase constants of TM wave 2 is considerable regardless of the frequency and the TM width. We can also understand that OHCs affect the phase constants of TM wave 2 more strongly when $f = 5$ kHz. Fig. 3(c) indicates that the influence of OHCs on the attenuation constants of TM wave 1 is stronger than the one on the phase constants in any case of the TM width. We can also understand that the influence becomes stronger as the TM width decreases. On the other hand, Fig. 3(d) shows that compared to TM wave 1, the attenuation constants of TM wave 2 are affected more strongly by OHCs, and the dependence on the TM width decreases.

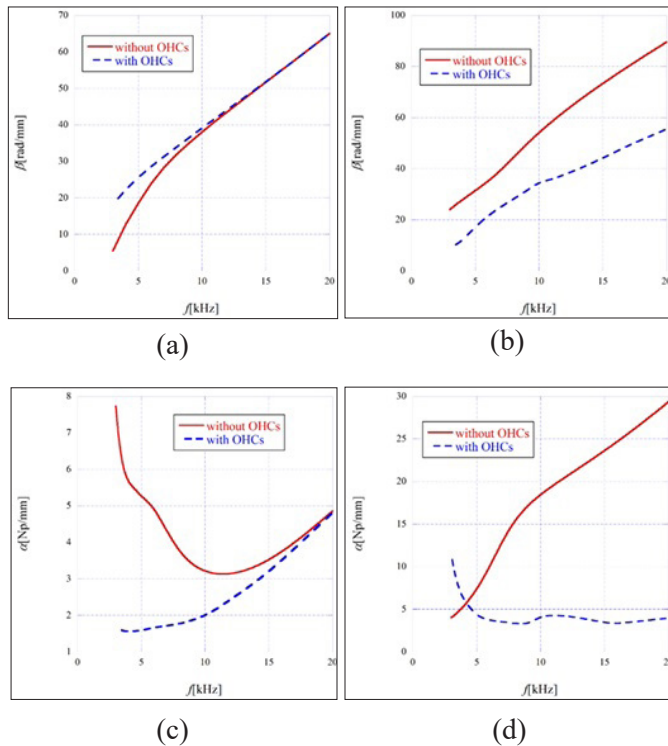


Fig. 2. Frequency characteristics of phase and attenuation constants.

Note: Phase constant of (a) TM wave 1 and (b) TM wave 2 and attenuation constant of (c) TM wave 1 and (d) TM wave 2 are shown.

Conclusion

This study investigated the influence of OHCs on the propagation characteristics of two types of TM waves—TM wave 1 and TM wave 2—by employing modal analysis using finite element method-based software.

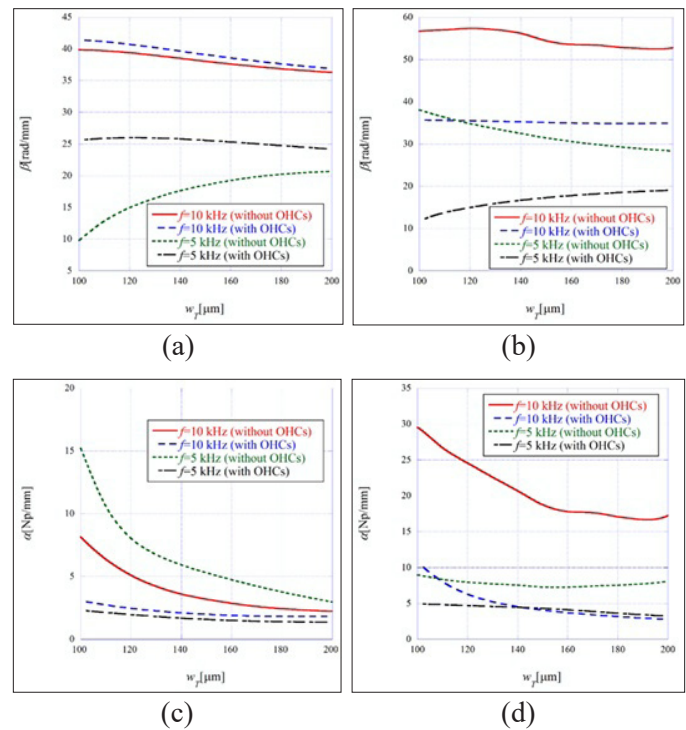


Fig. 3. Phase and attenuation constants as a function of TM width w_T .

Note: Phase constant of (a) TM wave 1 and (b) TM wave 2 and attenuation constant of (c) TM wave 1 and (d) TM wave 2 are shown.

For TM wave 1, the concentration in the limbal attachment zone and the subsequent diminishing influence of OHCs at higher frequencies suggest a small influence from OHCs. On the other hand, TM wave 2, with its concentration at the tip of the TM main body, experiences a more pronounced impact from OHCs across all frequency domains, especially in the high-frequency range. The examination of phase and attenuation constants with varying TM widths indicates noteworthy trends. The influence of OHCs on TM wave 1 is more pronounced in the attenuation constants than in the phase constants, particularly at lower frequencies and smaller TM widths. In contrast, for TM wave 2, the attenuation constants are affected more strongly by OHCs than by TM wave 1, and the dependence on TM width decreases. This research contributes valuable insights into the intricate interplay between OHCs and TM waves, shedding light on their roles in cochlear mechanics and hearing sensitivity.

Competing Interests

The authors declare that they have no competing interests.

References

1. Spector AA, Brownell WE, Popel AS. Mechanical and electromotile characteristics of auditory outer hair cells. *Med*

- Biol Eng Comput. 1999 Mar;37(2):247-51. doi: 10.1007/BF02513294. PMID: 10396830.
2. Tolomeo JA, Steele CR, Holley MC. Mechanical properties of the lateral cortex of mammalian auditory outer hair cells. *Biophys J*. 1996 Jul;71(1):421-9. doi: 10.1016/S0006-3495(96)79244-5. PMID: 8804625; PMCID: PMC1233493.
3. Karavitaki KD, Mountain DC. Imaging electrically evoked micromechanical motion within the organ of corti of the excised gerbil cochlea. *Biophys J*. 2007 May 1;92(9):3294-316. doi: 10.1529/biophysj.106.083634. Epub 2007 Feb 2. PMID: 17277194; PMCID: PMC1852364.
4. Dewey JB, Xia A, Müller U, Belyantseva IA, Applegate BE, Ogghalai JS. Mammalian Auditory Hair Cell Bundle Stiffness Affects Frequency Tuning by Increasing Coupling along the Length of the Cochlea. *Cell Rep*. 2018 Jun 5;23(10):2915-2927. doi: 10.1016/j.celrep.2018.05.024. PMID: 29874579; PMCID: PMC6309882.
5. Furness DN, Mahendrasingam S, Ohashi M, Fettiplace R, Hackney CM. The dimensions and composition of stereociliary rootlets in mammalian cochlear hair cells: comparison between high- and low-frequency cells and evidence for a connection to the lateral membrane. *J Neurosci*. 2008 Jun 18;28(25):6342-53. doi: 10.1523/JNEUROSCI.1154-08.2008. PMID: 18562604; PMCID: PMC2989617.
6. Aranyosi AJ, Freeman DM. Sound-induced motions of individual cochlear hair bundles. *Biophys J*. 2004 Nov;87(5):3536-46. doi: 10.1529/biophysj.104.044404. Epub 2004 Aug 17. PMID: 15315953; PMCID: PMC1304819.
7. Kitamura T. Mode analysis of tectorial membrane in cochlea. *Biomedical and Pharmacology Journal*. 2021; 14: 1389–1395. doi: 10.13005/bpj/2241
8. Kitamura T, Ueno T. Attenuation characteristics of tectorial membrane wave. *Akustika*. 2022; 43: 60-64.
9. Ni G, Elliott SJ, Baumgart J. Finite-element model of the active organ of Corti. *J R Soc Interface*. 2016 Feb;13(115):20150913. doi: 10.1098/rsif.2015.0913. PMID: 26888950; PMCID: PMC4780563.
10. Gan RZ, Reeves BP, Wang X. Modeling of sound transmission from ear canal to cochlea. *Ann Biomed Eng*. 2007 Dec;35(12):2180-95. doi: 10.1007/s10439-007-9366-y. Epub 2007 Sep 18. PMID: 17882549.
11. Koike T, Sakamoto C, Sakashita T, Hayashi K, Kanzaki S, Ogawa K. Effects of a perilymphatic fistula on the passive vibration response of the basilar membrane. *Hear Res*. 2012 Jan;283(1-2):117-25. doi: 10.1016/j.heares.2011.10.006. Epub 2011 Nov 15. PMID: 22115725.
12. De Paolis A, Bikson M, Nelson JT, de Ru JA, Packer M, Cardoso L. Analytical and numerical modeling of the hearing system: Advances towards the assessment of hearing damage. *Hear Res*. 2017 Jun;349:111-128. doi: 10.1016/j.heares.2017.01.015. Epub 2017 Feb 2. PMID: 28161584; PMCID: PMC7000179.

***Corresponding author:** Professor Toshiaki Kitamura, Kansai University, Osaka, Japan. E-mail: kita@kansai-u.ac.jp